



Cite this: *RSC Adv.*, 2023, **13**, 14102

## **$\beta$ -Ketoadipic acid production from poly(ethylene terephthalate) waste via chemobiological upcycling†**

Sang-Mook You,<sup>a</sup> Si Seon Lee,<sup>b</sup> Mi Hee Ryu,<sup>c</sup> Hye Min Song,<sup>d</sup> Min Soo Kang,<sup>a</sup> Ye Jean Jung,<sup>a</sup> Eun Chae Song,<sup>e</sup> Bong Hyun Sung,<sup>f</sup> Si Jae Park,<sup>d</sup> Jeong Chan Joo, <sup>\*b</sup> Hee Taek Kim<sup>\*e</sup> and Hyun Gil Cha <sup>\*a</sup>

The upcycling of poly(ethylene terephthalate) (PET) waste can simultaneously produce value-added chemicals and reduce the growing environmental impact of plastic waste. In this study, we designed a chemobiological system to convert terephthalic acid (TPA), an aromatic monomer of PET, to  $\beta$ -ketoadipic acid ( $\beta$ KA), a C6 keto-diacid that functions as a building block for nylon-6,6 analogs. Using microwave-assisted hydrolysis in a neutral aqueous system, PET was converted to TPA with Amberlyst-15, a conventional catalyst with high conversion efficiency and reusability. The bioconversion process of TPA into  $\beta$ KA used a recombinant *Escherichia coli*  $\beta$ KA expressing two conversion modules for TPA degradation (*tphAabc* and *tphB*) and  $\beta$ KA synthesis (*aroY*, *catABC*, and *pcaD*). To improve bioconversion, the formation of acetic acid, a deleterious factor for TPA conversion in flask cultivation, was efficiently regulated by deleting the *poxB* gene along with operating the bioreactor to supply oxygen. By applying two-stage fermentation consisting of the growth phase in pH 7 followed by the production phase in pH 5.5, a total of 13.61 mM  $\beta$ KA was successfully produced with 96% conversion efficiency. This efficient chemobiological PET upcycling system provides a promising approach for the circular economy to acquire various chemicals from PET waste.

Received 31st March 2023  
 Accepted 2nd May 2023

DOI: 10.1039/d3ra02072j  
[rsc.li/rsc-advances](http://rsc.li/rsc-advances)

## Introduction

Increasing awareness of environmental issues has inspired an intensified search for novel solutions to counteract the accumulation of plastic waste in landfills and oceans.<sup>1,2</sup> One contributor to plastic pollution is polyethylene terephthalate (PET), which is produced at a rate of 70 million tons annually and widely used in single-use packaging. In line with carbon-neutral policies and a circular economy approach, strategies

for the upcycling of PET waste have gained increasing attention for their potential in reducing pollution and minimizing carbon dioxide emissions. When estimating the cost of recycled terephthalic acid (rTPA) sourced from conventional chemical recycling process of PET waste, the potential production costs of rTPA would be \$1.93 per kg after production of rTPA with 69–83% less greenhouse gas (GHG) emissions but at a higher cost. Hence it is needed for further development in cost reduction. Suggesting further development in cost reduction.<sup>3,4</sup>

To address the problem, several upcycling methods have been suggested, including chemical, biological, and chemobiological upcycling. While enzymatic hydrolysis offers a promising biotechnological approach to PET degradation under mild conditions, but it has serious limitations, such as the prerequisite for amorphous or low-crystallinity PET necessary for the proper enzyme activity.<sup>5</sup> Recently, a combination of chemical depolymerization of PET and biological upcycling of TPA have been developed to produce value-added chemicals such as protocatechuic acid (PCA), gallic acid, pyrogallol, catechol, muconic acid, and vanillic acid. These chemicals have various industrial applications and can be produced through whole-cell bioconversion.<sup>4–8</sup>

Chemical depolymerization processes of PET, such as glycolysis, methanolysis, aminolysis, and hydrolysis have all been extensively studied and vary by the type of reagent used.<sup>9</sup>

<sup>a</sup>Center for Bio-based Chemistry, Korea Research Institute of Chemical Technology (KRICT), Ulsan 44429, Republic of Korea

<sup>b</sup>Department of Biotechnology, The Catholic University of Korea, Bucheon-si, Gyeonggi-do 14662, Republic of Korea. E-mail: jcjoo@catholic.ac.kr

<sup>c</sup>Green Carbon Research Center Korea Research Institute of Chemical Technology (KRICT), Daejeon 34114, Republic of Korea

<sup>d</sup>Department of Chemical Engineering and Materials Science, Graduate Program in System Health Science & Engineering, Ewha Woman's University, Seoul 03760, Republic of Korea

<sup>e</sup>Department of Food Science and Technology, College of Agriculture and Life Sciences, Chungnam National University, Daejeon 34134, Republic of Korea. E-mail: heetaek@cnu.ac.kr

<sup>f</sup>Synthetic Biology Research Center, Korea Research Institute of Bioscience and Biotechnology, Daejeon 34141, Republic of Korea

† Electronic supplementary information (ESI) available: Image of plastic sample, NMR of TPA from PET hydrolysis details. See DOI: <https://doi.org/10.1039/d3ra02072j>



Particularly, the hydrolysis process can directly produce TPA by cleavage of ester bonds in the PET chain in acidic or basic aqueous conditions without an organic solvent, thereby increasing the energy economy and allowing its direct utilization as the substrate for bioconversion. Microwave radiation can be further employed in hydrolysis to reduce the thermodynamic kinetic energies in PET depolymerization under mild conditions.<sup>4</sup> For being energy effective, the hydrolysis reaction should incorporate a heterogenous catalyst with an active surface group that functions as Lewis/Brønsted acids and bases along with an easily recoverable rigid framework. Accordingly, Amberlyst-15, a sulfonic acid-based styrene-divinylbenzene copolymer, is used to catalyze a variety of acidic reactions such as esterification, phenol alkylation, and condensation, and can also be used for hydrolysis.<sup>10</sup> Furthermore, Amberlyst-15's rigid non-corrosive macroporous structure provides physical and chemical stability allowing its recovery from the reaction solution *via* filtration and centrifugation.<sup>11</sup>

The biological upcycling process of monomers hydrolyzed from PET can be accomplished using a whole-cell microbial catalyst suitably constructed. Because of its ease of manipulation, culturing, and scalability, *Escherichia coli* (*E. coli*) is the most well-established production host strain in the cell factory fields.<sup>12</sup> To initiate bioconversion, the substrates should not be toxic to microbial cells and should be able to pass through the cell membrane into the cytoplasmic space in the culture media, under suitable pH conditions. However, the bioconversion of TPA is limited by its potential toxicity which affects biocatalyst growth and metabolism capacity, and by its absolute concentration in reaction media resulting from the low solubility. In a previous study, TPA inhibited bioconversion and reduced the yield of a biocatalytic reaction by over 1 g L<sup>-1</sup>.<sup>5</sup> Therefore, overcoming the TPA-induced inhibition is crucial to develop an efficient biological upcycling process with sustainability.

In this study, we present a chemobiological approach for producing  $\beta$ -ketoadipic acid ( $\beta$ KA) from PET waste. To validate our proposed system for  $\beta$ KA production, we utilized an actual disposable plastic coffee cup to establish proof-of-concept, as experiments conducted solely with reagents would not be sufficient to demonstrate real-world applicability. Our approach involves hydrolysis of PET using Amberlyst-15 (as shown in Fig. 1) under microwave conditions, followed by bioconversion with *E. coli* strains that overexpress enzymes involved in the  $\beta$ KA synthesis pathway. We chose to use the commercially available and cost-effective acidity catalyst, Amberlyst-15, to showcase the practicality of our system in industrial settings. To develop an efficient biological upcycling process and a TPA fed-batch conversion system, we profiled TPA conversion to identify deleterious factors under flask culturing conditions. Acetic acid accumulation, the critical deleterious factor for conversion, was controlled by deleting the acetate-forming gene (*poxB*) from the *E. coli* strain and modulating the dissolved oxygen (DO) level in the bioreactor. Finally, after determining the optimal pH for TPA transportation into the cytoplasm to improve substrate availability and enhance the bioconversion rate, a two-stage fed-batch bioconversion system was successfully developed. The proposed sequential waste PET upcycling composed of

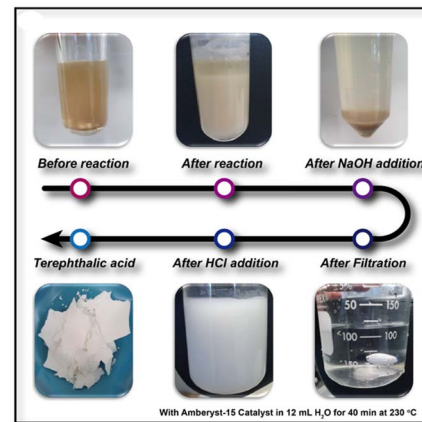


Fig. 1 Schematic illustration of the preparation of TPA from PET using the acidic catalyst, Amberlyst-15.

industrial catalyst-based PET depolymerization and followed by easily scalable whole-cell catalyst, *E. coli* strain-based  $\beta$ KA production, would be enabling a plastic circular economy.

## Experimental

### Materials

Amberlyst-15 and barium chloride ( $\text{BaCl}_2$ ) were purchased from Sigma-Aldrich (St. Louis, MO, USA). Sulfuric acid ( $\text{H}_2\text{SO}_4$ ) was acquired from Samchun Chemicals (Seoul, Korea). *E. coli* XL1-Blue competent cells were purchased from Stratagene (La Jolla, CA). The genes used for plasmid construction were obtained through gene synthesis by Cure Bio (Seoul, Korea).

### Activation of Amberlyst-15

The activation of Amberlyst-15 was performed as previously described, with a slight modification.<sup>12</sup> Amberlyst-15 was ground to a fine powder and activated in sulfuric acid for 3 h at 25 °C. The activated Amberlyst-15 was filtered and washed with double distilled water (DIW) several times until no sulfate was detected in the supernatant using a  $\text{BaCl}_2$  solution.<sup>13</sup>

### Microwave-assisted PET hydrolysis with Amberlyst-15

Microwave-assisted PET hydrolysis was performed using a microwave reaction system (Monowave 400, Anton Paar, Austria) equipped with temperature and pressure sensors. We added 0.1 g of PET powder to the reactor and 12 mL DIW containing 0.1 g of Amberlyst-15. To determine the optimal conditions for PET hydrolysis, we measured the reaction yields at various catalyst amounts (0.01 g, 0.05 g, and 0.1 g) and reaction times (10, 20, 30, 40, and 50 min) at 505 K. After the reaction, the produced TPA was purified using the following method. The solution was filtered to separate ethylene glycol (EG) from the reaction solution, and the solid residues were washed separately with 1 M NaOH to dissolve the produced TPA in the form of disodium-TPA ( $\text{Na}_2\text{-TPA}$ ). The  $\text{Na}_2\text{-TPA}$  was then recrystallized by adding twice the equivalent amount of 2 M HCl solution. The resulting white precipitate was filtered, dried, and



the filtered catalysts were reused for the above reaction. The PET conversion rate (%) and TPA yield (%) were calculated as follows:<sup>4</sup>

synthesized *aroY* was digested with *BamHI* and *SbfI* before being ligated into pKA312 and digested with the same restriction enzymes. All cloned DNA was transferred into *E. coli* XL1-Blue cells and grown in LB medium at 37 °C with shaking at 200 rpm.

$$\text{PET conversion (\%)} = \frac{\text{consumed amount of PET after reaction (g)}}{\text{initial amount of PET (g)}} \times 100 (\%) \quad (1)$$

$$\begin{aligned} \text{TPA yield (\%)} &= \frac{\text{experimentally produced TPA amount (g)}}{\text{theoretically produced TPA amount (g)}} \times 100 (\%) \\ &= \frac{\text{produced TPA amount (g)}}{\frac{\text{degraded PET amount (g)} \times 163.13 \text{ (g mol}^{-1})}{192.2 \text{ (g mol}^{-1})}} \times 100 (\%) \end{aligned} \quad (2)$$

### Bacterial strains, plasmids, and culture conditions

All bacterial strains and plasmids used in this study are listed in Table 1. Cloning, whole-cell bioconversion, and fermentation were performed using *E. coli* XL-1 Blue. *E. coli* was grown in Luria-Bertani (LB) medium containing 10 g L<sup>-1</sup> tryptone, 5 g L<sup>-1</sup> yeast extract, and 10 g L<sup>-1</sup> NaCl at 37 °C with shaking at 200 rpm.

### Construction of *E. coli* strain for βKA production

Gene cloning was performed using the vectors pKE112, pKM212, and pKA312 which are listed in Table 2. The TPA degradation module (pKM212 vector) was used to convert TPA to TPA-1,2-cis-dihydro diol and further to PCA. The PCA decarboxylation-encoded *AroY* enzyme for PCA conversion to catechol was inserted into the pKA312 vector.<sup>5</sup> The cat operon genes for catechol-1,2-dioxygenase (*CatA*), muconate cyclo-isomerase (*CatB*), and muconolactone D isomerase (*CatC*), as well as *PcaD*, were inserted into the pKE112 vector to generate βKA from catechol through meta-cleavage.<sup>14</sup> For pKE112-catABCpcaD, DNA fragments from each gene were cloned sequentially using *EcoRI*, *KpnI*, *BamHI*, *SbfI*, and *HindIII* restriction enzymes.<sup>15</sup> pKM212-tphBAabc was also created by inserting four genes into five restriction enzyme sites. The

### Cultivation and fermentation

*E. coli* XL1-Blue with appropriate plasmids was grown overnight in 2 mL LB medium at 37 °C and 220 rpm. The culture was transferred to a 250 mL baffled flask with 25 mL of minimal medium containing 5 g L<sup>-1</sup> glucose and 10 g L<sup>-1</sup> glycerol as a complex carbon source and 3 mM TPA as a substrate. Cultivation was carried out for 72 h at 30 °C, with samples taken every 24 h for analysis. Fermentation was carried out in a 2.5 L bioreactor (BioCNS, Daejeon, Korea) with a working volume of 500 mL. A volume of 4 mL of culture was prepared as described, in the baffled flask and added to a minimal medium containing the same concentrations of substrates to obtain an initial optical density (OD) of 30 at 600 nm. Fermentation was carried out at 30 °C and 600 rpm; the agitation speed was adjusted to maintain a level of DO above 30%. When its concentration dropped to 5 g L<sup>-1</sup>, glycerol was added as part of a solution containing minimal medium, and the pH was adjusted to 5.5 with a solution containing 28% (v/v) ammonia.

### Analytical procedures

Attenuated total reflection Fourier transform infrared (ATR-FT-IR) spectra of Amberlyst-15 were recorded before and after the catalytic reaction region within 4000–400 cm<sup>-1</sup> using an FTIR

Table 1 Primers used in this study

Genes	Forward and reverse primers	Source strain	Ref.
<i>catA</i>	F: GAATTCCATGACCGTGAATAATTCCCACAC R: GGTACCTCAGCCCTCCTGCAACGC	<i>Pseudomonas putida</i> KT2440	This study
<i>catB</i>	F: GGTACCTTTCACACAGGAAACAGACCATGACAAGCGTGTGATTGAAC R: GGATCCTCAGCGACGGCGAAGC	<i>Pseudomonas putida</i> KT2440	This study
<i>catC/pcaD</i>	F: GGATCCTTTCACACAGGAAACAGACCATGTTGTTCCACGTGAAGATGAC R: AAGCTTTAGTGAGCCAGCAGG	<i>Pseudomonas putida</i> KT2440	This study
<i>aroY</i>	F: GGATCCATGCAGAACCCGATCACGGA R: CCTGCAGGTTACTTCTGTCGCTGAACCA	<i>Klebsiella pneumoniae</i>	This study
<i>tphB</i>	Gene synthesis at IDT	<i>Comamonas</i> sp. E6	1
<i>tphA<sub>abc</sub></i>	Gene synthesis at IDT	<i>Comamonas</i> sp. E6	1



Table 2 Characteristics of bacterial strains and plasmids used in this study

Strain and plasmid	Characteristics of the strain and plasmid	Ref.
<b>Strains</b>		
<i>E. coli</i> DH5 $\alpha$	$F^-$ (80d <i>lacZ</i> M15) ( <i>lacZYA-argF</i> ) U169 <i>hsdR17(r-m+)</i> <i>recA1 endA1 relA1 deoR</i>	Real biotech
<i>E. coli</i> XL1-Blue	<i>recA1 endA1 gyrA96 thi-1 hsdR17 supE44 relA1 lac</i> [FA1proAB <i>lacI'ZΔM15</i> Tn10 (Tet <sup>R</sup> )]	Stratagene
<i>E. coli</i> XL1-Blue <i>ΔpoxB</i>	<i>E. coli</i> XL1-Blue <i>ΔpoxB</i>	
<i>E. coli</i> $\beta$ KA	<i>E. coli</i> XL1-Blue harboring pKE112CatABCpcaD, pKM212TphAB <sub>abc</sub> and pKA312AroY	This study
<i>E. coli</i> $\beta$ KA ( <i>ΔpoxB</i> )	<i>E. coli</i> XL1-Blue <i>ΔpoxB</i> harboring pKE112CatABCpcaD, pKM212TphAB <sub>abc</sub> and pKA312AroY	This study
<b>Plasmids</b>		
pKE112CatABCpcaD	pKE112; <i>P<sub>lac</sub></i> promoter, <i>Pseudomonas putida</i> KT2440 <i>catABC</i> and <i>pcaD</i> genes, Amp <sup>R</sup>	This study
pKM212TphBA <sub>abc</sub>	pKM212; <i>P<sub>lac</sub></i> promoter, <i>Comamonas</i> sp. E6 <i>tphB</i> and <i>tphA<sub>abc</sub></i> genes, Km <sup>R</sup>	This study
pKA312AroY	pKA31212; <i>P<sub>lac</sub></i> promoter, <i>Enterobacter cloacae</i> <i>aroY</i> , Cm <sup>R</sup>	This study

spectrometer (Thermo Fisher Scientific Nicolet is50, USA) equipped with a smart iTR diamond/ZnSe ATR accessory. The TPA hydrolysate structure was confirmed with <sup>1</sup>H NMR spectroscopy using an AVANCE III 400 MHz spectrometer (Bruker Biospin, Rheinstetten, Germany). A spectrophotometer was used to measure the OD of the cells at 600 nm (Shimadzu, Japan). High-performance liquid chromatography (Agilent Technologies, Santa Clara, CA, USA) was used to determine the concentrations of substrates and products within the culture. TPA levels were determined using a C18 column (Rstech, Daejeon, Korea) at 30 °C with an eluent containing a 9 : 1 mixture of water and acetonitrile and, 0.1% trifluoroacetic acid at a flow rate of 1 mL min<sup>-1</sup>. TPA was detected using a variable-wavelength detector at 254 nm. At 50 °C, glucose, glycerol, acetic acid, and  $\beta$ KA were separated on an Aminex HPX-87H column (300 × 7.8 mm, Bio-Rad Laboratories, Hercules, CA, USA). The mobile phase was 5 mM sulfuric acid at a flow rate of 0.8 mL min<sup>-1</sup>, and compounds were detected using a refractive index detector with the following retention times: 6.5 minutes for glucose, 8.3 minutes for  $\beta$ KA, 9.7 minutes for glycerol, and 11.1 minutes for acetic acid.

## Results and discussion

### Production of TPA by microwave-assisted PET hydrolysis with Amberlyst-15

We chose the PET waste model as a clear plastic disposable coffee cup to verify the ability of our proposed chemobiological PET upcycling system. The coffee cups were cut into small squares with dimensions of 1 × 1 and then grounded using a SPEX 6857D Freezer/Mill to obtain a powdered form for efficient hydrolysis (Fig. S1†). To hydrolyse the grounded PET powder in DI water without any additives under microwave irradiation, we employed the commercial heterogeneous catalyst Amberlyst-15, which has an active surface sulfonate group that promotes acidity (as shown in Fig. 2a). The use of microwave heating during hydrolysis facilitated the transfer of heat to specific regions of PET, thereby accelerating degradation and potentially reducing the required reaction kinetic energy. The yield of TPA from PET was calculated to confirm the feasibility of the method and optimize the reaction conditions using Amberlyst-15. With increasing amounts of catalyst, the

corresponding Brønsted acidic sites in the sulfonate group increased the level of hydroxonium ions, which in turn induced the nucleophilic attack of water on PET for depolymerization into TPA (Fig. 2b).<sup>4</sup> During the initial 10 min of the reaction, the efficiency of PET hydrolysis was constant; however, after 40 min, it increased linearly in time until it reached saturation at about 100% conversion efficiency. The initial pause in the reaction might be due to the random chain scission of PET, while the participation of depolymerized TPA accelerated the rate of the reaction (Fig. 2c).<sup>16</sup> In this study, we investigated the proposed chemobiological upcycling of hydrolysate TPA into high purity  $\beta$ KA. To achieve this, we filtered the solution for ethylene glycol (EG) that had also degraded from the PET granules. NMR spectroscopy confirmed the production of TPA by Amberlyst-15-mediated PET hydrolysis. The hydrolysate showed two main peaks representing aromatic single protons and hydroxyl protons at 8.03 and 13.31 ppm, respectively (Fig. S2†). We found that Amberlyst-15 could be easily recovered from the reaction solution by simple filtration and used up to the 4th cycle with a conversion efficiency of over 80% (Fig. 2d). We compared the FT-IR spectra of Amberlyst-15 at the first and 4th reaction to determine the state of the surface functional group (Fig. 2e). The characteristic peaks of the catalyst after the 4th round of

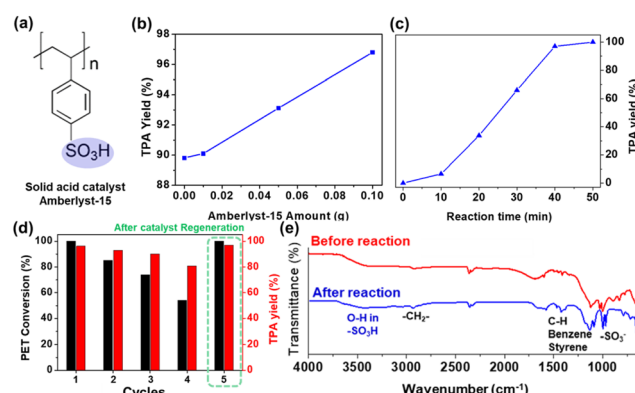


Fig. 2 (a) Chemical structure of Amberlyst-15 (b) and (c) TPA yield over catalyst amount and reaction time, respectively (d) recyclability and efficiency of the catalyst after regeneration by immersion in sulfuric acid (e) FT-IR spectra of Amberlyst-15 before (red) and after (blue) hydrolysis of PET.



reaction was comparable to those of the pure catalyst, except in the region 3500–3300  $\text{cm}^{-1}$  around the peak at 3425  $\text{cm}^{-1}$  corresponding to the O–H region in the sulfonate group.<sup>17</sup> Microwave radiation only affects the energy transfer during PET depolymerization, but has a negligible effect on the functional groups present on the surface of the Amberlyst-15 catalyst until its fourth reusability. To regenerate the sulfonate groups on the outer surface of the catalyst, we treated it with sulfuric acid, which unlocked the sulfonate groups and restored the catalytic efficiency of Amberlyst-15 to its initial state, as shown in Fig. 2e. The recoverable catalytic efficiency of Amberlyst-15 under the microwave irradiation following this simple treatment with sulfuric acid can increase energy efficiency.

### Development of a biological upcycling process for $\beta$ KA from TPA

Building on our previous efforts to produce value-added aromatic monomers from PCA as a precursor, we designed artificial pathways composed of a TPA degradation module (pKM212 vector) for PCA production and a  $\beta$ KA synthesis module (pKA312 and pKE112 vector), a three-vector system overexpressing the enzymes needed for an effective PCA conversion (Fig. 3).<sup>18</sup> *E. coli* XL1-Blue expressing these vectors (*E. coli*  $\beta$ KA hereafter) was used to produce  $\beta$ KA from the substrate hydrolysate TPA in the presence of carbon sources such as glucose for initial cell growth and glycerol to supply redox potential for TPA conversion. The main carbon source used in this study was glycerol, which is a major byproduct of the biodiesel industry. The surplus amount of crude glycerol produced can cause environmental issues, and thus, there is a demand to utilize it efficiently. Flask cultivations of *E. coli*  $\beta$ KA were repeatedly conducted to identify potentially deleterious factors hindering the biological upcycling process. We found that all enzymes encoded in *E. coli*  $\beta$ KA were expressed, enabling the successful conversion of TPA into  $\beta$ KA with a 98% molar yield, as shown in Fig. 4. Furthermore, the rate of TPA conversion was boosted in parallel with the activation of glycerol metabolism, indicating a correlation between glycerol consumption and  $\beta$ KA bioconversion. However, glycerol was slowly metabolized and was still present at the end of the conversion reaction. Because glycerol enters *E. coli* cells passively *via* the *GlpF* glycerol facilitator protein, where it undergoes anaerobic metabolism to produce the glycolytic intermediate dihydroxyacetone phosphate, we postulated that the delayed glycerol consumption in the flask cultures of recombinant *E. coli* could be attributed to

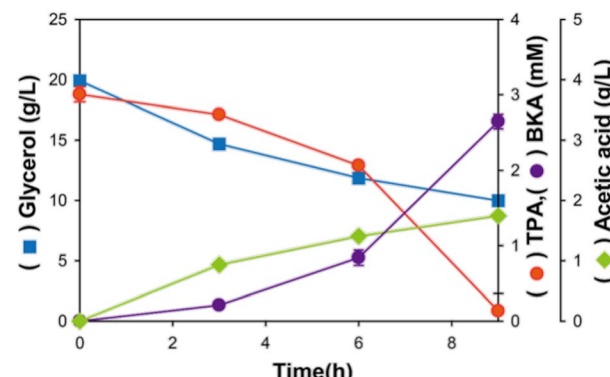


Fig. 4 Flask cultivation profiling by *E. coli*  $\beta$ KA in a minimal medium containing TPA as the substrate and glucose and glycerol as carbon sources for  $\beta$ KA production containing TPA as the substrate and glucose and glycerol as carbon sources for  $\beta$ KA production. All cultivations were done in duplicates.

the limited oxygen level. From these observations, we hypothesized that the TPA conversion rate could be enhanced by improving glycerol metabolism. Furthermore, the steady accumulation of acetic acid as a byproduct was also observed, its concentration reaching 0.9 mM at the end of the reaction. Acetic acid is a potentially toxic compound, having deleterious effects on cell fitness by decreasing intracellular pH and leading to metabolic perturbation. Thus, its accumulation results in low bioconversion efficiency and should be appropriately regulated.<sup>19</sup> Taken together, bioconversion profiling of TPA in *E. coli*  $\beta$ KA indicated that improving glycerol metabolism as well as properly regulating acetic acid accumulation could be critical in developing a fed-batch conversion system to produce  $\beta$ KA.

### Improved biological upcycling process of $\beta$ KA from TPA by controlling deleterious factors

To support oxidative glycerol respiration, bioconversion of TPA into  $\beta$ KA was performed using *E. coli*  $\beta$ KA in a bioreactor with supplied oxygen (dissolved oxygen, DO level of 30%). As a result, glycerol metabolism was improved, and a total of 36 g  $\text{L}^{-1}$  glycerol was consumed, which is 3 times higher than that in the flask cultivation (12 g  $\text{L}^{-1}$ ). However, 4 g  $\text{L}^{-1}$  acetic acid was synthesized, which is 5 times higher than that in shaking flask cultivation (Fig. 5a). Additionally, 0.5 mM TPA was not entirely converted into  $\beta$ KA until the end of the bioconversion reaction, even though the initial TPA conversion rate was improved compared to that in the shaking flask cultivation. Under flask cultivation conditions, glycerol metabolism can easily switch from oxidative respiration to fermentative metabolism, resulting in an excess of nicotinamide adenine dinucleotide hydrogen (NADH). Therefore, fermentative glycerol metabolism generates enough NADH pools to support the initial TPA conversion. However, because the bioconversion of TPA into PCA occurs in a self-compensated manner, fermentative metabolism may trigger an intrinsic redox imbalance, leading to the formation of byproducts such as acetic acid to replenish NAD<sup>+</sup> content. Consequently, exposure to the toxic organic acid could

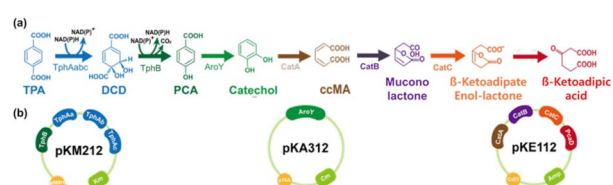


Fig. 3 Schematic illustrations of (a) the bioconversion pathway of TPA to  $\beta$ KA in the *E. coli*  $\beta$ KA strain and (b) expression vectors to construct  $\beta$ KA biosynthetic pathway from TPA.



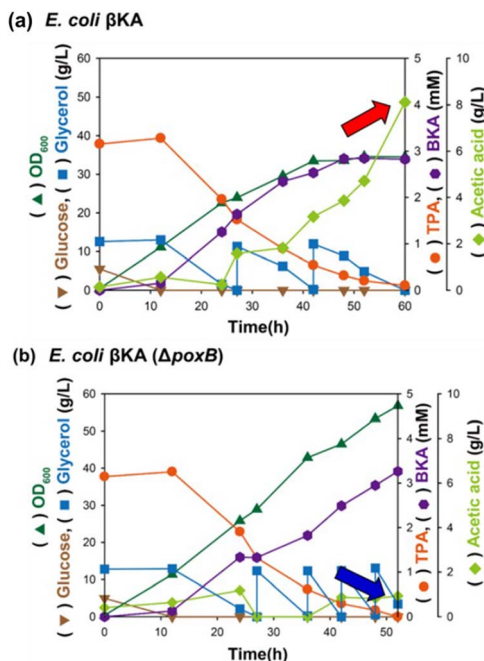


Fig. 5 Bioconversion of TPA into  $\beta$ KA in (a) *E. coli*  $\beta$ KA and (b) *E. coli*  $\beta$ KA ( $\Delta$ poxB) at a 30% DO level with stepwise glycerol feeding. The red and blue arrows indicate the accumulation of acetic acid, respectively. All fermentations were done in duplicates.

deteriorate cell fitness and hinder bioconversion. We hypothesized that improved glycerol metabolism in the bioreactor induced the excessive formation of pyruvate or acetyl-CoA, which are precursors of acetic acid, leading to increased acetic acid formation. The accumulated acetic acid negatively affected the bioconversion of TPA into  $\beta$ KA. Therefore, they deleted the acetic acid-forming gene to regulate the acetic acid formation and improve TPA bioconversion into  $\beta$ KA. *E. coli* strains have three independent acetate-producing pathways: phosphotransacetylase (*Pta*), acetate kinase (*AckA*), acetyl-CoA synthetase (*Acs*), and pyruvate oxidase (*PoxB*). In the *E. coli* strain, *PoxB* only catalyzes the irreversible conversion of pyruvate into acetic acid, unlike the other acetic acid-forming genes. Thus, the *poxB* gene was deleted to regulate acetic acid production and improve the efficacy of  $\beta$ KA production, and *E. coli*  $\beta$ KA ( $\Delta$ poxB) was further constructed. In the presence of *E. coli*  $\beta$ KA ( $\Delta$ poxB) at a DO level of 30%, TPA bioconversion led to a dramatically reduced acetic acid accumulation—below  $0.94\text{ g L}^{-1}$ , which was 4.2-fold lower than that measured when using *E. coli*  $\beta$ KA (Fig. 5b). In addition, *E. coli*  $\beta$ KA ( $\Delta$ poxB) improved bioconversion, as  $3.26\text{ mM}$   $\beta$ KA was synthesized from TPA with a 100% molar conversion yield. Thus, deletion of *poxB* gene efficiently regulated the acetic acid metabolism and reduced its accumulation enhancing bioconversion of TPA into  $\beta$ KA. The steady increase in cell growth and rates of glycerol consumption during bioconversion can be regarded as positive parameters indicating that *E. coli*  $\beta$ KA ( $\Delta$ poxB) could be applied for fed-batch bioconversion to maximize the production of  $\beta$ KA. However, the slow TPA conversion rate can be regarded as a negative parameter of the fed-batch bioconversion of TPA into  $\beta$ KA, indicating that TPA

was not participating in the TPA conversion owing to poor transportation into the cytoplasmic space.

### $\beta$ KA production enhancement by two-stage fed-batch bioconversion

In neutral pH ( $\approx 7$ ), optimal for favourable bacterial growth, charge repulsion might occur between the aromatic carboxylic groups in the substrate and phosphate groups in the outer membrane of Gram-negative bacteria.<sup>21,24</sup> TPA, one of the aromatic carboxylates, exists as a negatively charged ion; thus, the bacterial membrane may prevent its diffusion through the surface of *E. coli*.<sup>22,23</sup> Instead, TPA uptake is known to occur in a moderate acid condition ( $<6$ ) because carboxylic groups protonate allowing the passive diffusion of TPA through the bacterial membrane.<sup>20</sup> Therefore, considering the final pH of 5.5 at the end of the flask cultivation shown in Fig. 4 is consistent with the conditions required for maintaining *E. coli* strain viability, we designed a two-stage bioconversion process. Initially, appropriate *E. coli*  $\beta$ KA ( $\Delta$ poxB) was grown at pH 7 to express the relevant enzyme for the bioconversion of TPA into  $\beta$ KA. Then, pH was shifted from 7 to 5.5 to increase protonated TPA in reaction media and efficiently convert it to  $\beta$ KA.<sup>20</sup> At pH 5.5, the initial  $3.2\text{ mM}$  TPA conversion was terminated within 24 h, which was 2.1-fold faster than the sole conversion stage occurring at pH 7 (Fig. 6). Based on the increased reaction rate, TPA stepwise feeding was conducted using *E. coli*  $\beta$ KA ( $\Delta$ poxB). As a result, from a total TPA amount of  $14.13\text{ mM}$  with stepwise feeding of TPA, we produced  $13.61\text{ mM}$   $\beta$ KA; this corresponds to a 96% conversion rate at the end of fermentation. As a result of stepwise feeding of TPA, a total amount of  $14.13\text{ mM}$  TPA was used to produce  $13.61\text{ mM}$   $\beta$ KA, which corresponds to a 96% conversion rate at the end of fermentation. In addition, the two-stage fed-batch bioconversion system presented in this study exhibited comparable cell density ( $OD_{600} = 51$ ) to that used at pH 7 ( $OD_{600} = 56$ ). Collectively, our findings indicate that we have successfully constructed a chemobiological system for hydrolysing PET waste using Amberlyst-15 and biologically converting TPA into  $\beta$ KA. The synergistic effect of polar sulfonate

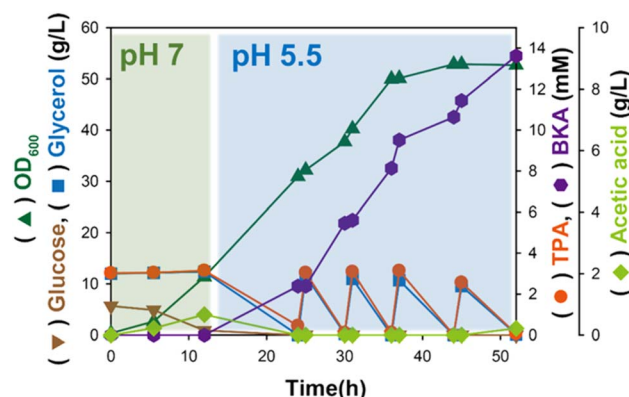


Fig. 6 Two-stage fed-batch bioconversion of TPA into  $\beta$ KA in *E. coli*  $\beta$ KA ( $\Delta$ poxB) under optimized conditions (pH 5.5 and 30% DO level) with stepwise TPA and glycerol feeding. Fed-batch fermentation was carried out once.

groups producing hydrogen ions and the non-corrosive matrix of Amberlyst-15 was clearly demonstrated in the high catalytic activity and reusability for producing the virgin monomeric component of actual plastic cups, TPA. Subsequently, TPA was used as a sequential substrate to produce  $\beta$ KA with high conversion efficiency using a recombinant *E. coli* strain with deletion of the related byproduct-producing gene under a two-stage fed-batch bioconversion process. However, the inherent issue of insufficient absolute glycerol utilization suggests that further research on glycerol utilization pathways in *E. coli* is required to enhance  $\beta$ KA production titers to levels that are suitable for industrial applications.

## Conclusions

In this study, we report a chemobiological upcycling strategy to produce  $\beta$ KA from PET waste. PET depolymerization into the TPA substrate was achieved by microwave-assisted hydrolysis with the heterogeneous acid catalyst Amberlyst-15. The sulfo-nate group of Amberlyst-15 was easily recovered by sulfuric acid treatment and showed 97% catalytic efficiency for TPA conversion. The fed-batch bioconversion of TPA into  $\beta$ KA was successfully developed by regulating acetic acid accumulation and applying two-stage bioconversion. The engineered *E. coli* (*E. coli*  $\beta$ KA ( $\Delta$ poxB)) developed in this study enabled the production of 13.61 mM  $\beta$ KA with a 96% conversion rate. Despite the successful development of the bioconversion system, several issues should be considered. First, the development of the bioconversion system may require operating high concentration TPA by chassis engineering, such as adaptive laboratory evolution. Next, introducing an efficient TPA transportation system, such as the TPA transporter system of TPA-degrading bacteria *Comamonas* sp. E6 may be also necessary. The proposed chemobiological system for the valorization of PET waste provides an innovative strategy to reduce the overall environmental impact of plastic-based industries by energy-efficient bioconversion.

## Author contributions

H. G. C., H. T. K., and J. C. J. designed the study. S. S. L., M. H. R., M. S. K. H. M. S., B. H. S., E. C. S., and Y. J. J. performed experiments on the chemobiological process for the production of  $\beta$ KA. S. M. Y. and S. J. P guided experiments and data interpretation. S. M. Y., H. T. K. and H. G. C. wrote the manuscript.

## Conflicts of interest

The author declares no conflict of interest.

## Acknowledgements

This research was supported by the Cooperative Research Program for Agriculture Science and Technology Development (PJ01708201 and PJ01708204) through the Rural Development Administration and the National Research Foundation of Korea (2022R1A4A1033015).

## References

- 1 M. J. Kang, H. T. Kim, M.-W. Lee, K.-A. Kim, T. U. Khang, H. M. Song, S. J. Park, J. C. Joo and H. G. Cha, *Green Chem.*, 2020, **22**, 3461–3469.
- 2 Y. Peng, P. Wu, A. T. Schartup and Y. Zhang, *Proc. Natl. Acad. Sci. U. S. A.*, 2021, **118**, e2111530118.
- 3 Y. Luo, E. Selvam, D. G. Vlachos and M. Ierapetritou, *ACS Sustainable Chem. Eng.*, 2023, **11**(10), 4209–4218.
- 4 A. Singh, N. A. Rorrer, S. R. Nicholson, E. Erickson, J. S. DesVeaux, A. F. T. Avelino, P. Lamers, A. Bhatt, Y. Zhang, G. Avery, L. Tao, A. R. Pickford, A. C. Carpenter, J. E. McGeehan and G. T. Beckham, *Joule*, 2021, **5**(9), 2479–2503.
- 5 N. F. S. Khairul Anuar, F. Huyop, G. Ur-Rehman, F. Abdullah, Y. M. Normi, M. K. Sabullah and R. Abdul Wahab, *Int. J. Mol. Sci.*, 2022, **23**, 12644.
- 6 H. T. Kim, M. Hee Ryu, Y. J. Jung, S. Lim, H. M. Song, J. Park, S. Y. Hwang, H.-S. Lee, Y. J. Yeon, B. H. Sung, U. T. Bornscheuer, S. J. Park, J. C. Joo and D. X. Oh, *ChemSusChem*, 2021, **14**, 4251–4259.
- 7 J. Mudondo, H.-S. Lee, Y. Jeong, T. H. Kim, S. Kim, B. H. Sung, S.-H. Park, K. Park, H. G. Cha, Y. J. Yeon and H. T. Kim, *J. Microbiol. Biotechnol.*, 2023, **33**, 1–14.
- 8 H. T. Kim, J. K. Kim, H. G. Cha, M. J. Kang, H. S. Lee, T. U. Khang, E. J. Yun, D.-H. Lee, B. K. Song, S. J. Park, J. C. Joo and K. H. Kim, *ACS Sustainable Chem. Eng.*, 2019, **7**, 19396–19406.
- 9 D. H. Kim, D. O. Han, K. In Shim, J. K. Kim, J. G. Pelton, M. H. Ryu, J. C. Joo, J. W. Han, H. T. Kim and K. H. Kim, *ACS Catal.*, 2021, **11**, 3996–4008.
- 10 H. Kim, S. Yang and D. H. Kim, *Environ. Res.*, 2020, **187**, 109667.
- 11 M. J. Kang, H. J. Yu, J. Jegal, H. S. Kim and H. G. Cha, *Chem. Eng. J.*, 2020, **398**, 125655.
- 12 D. Yang, S. Y. Park, Y. S. Park, H. Eun and S. Y. Lee, *Trends Biotechnol.*, 2020, **38**, 745–765.
- 13 H. Zhang, F. Tian, L. Xu, R. Peng, Y. Li and J. Deng, *Chem. Eng. J.*, 2020, **388**, 124214.
- 14 Y. Tian, H. Shen, Q. Wang, A. Liu, W. Gao, X.-W. Chen, M.-L. Chen and Z. Zhao, *Anal. Chem.*, 2018, **90**, 7843–7847.
- 15 S. Vasileiadis, C. Perruchon, B. Scheer, L. Adrian, N. Steinbach, M. Trevisan, P. Plaza-Bolaños, A. Agüera, A. Chatzinotas and D. G. Karpouzas, *Environ. Microbiol.*, 2022, 5105–5122.
- 16 J. E. Yang, J. W. Kim, Y. H. Oh, S. Y. Choi, H. Lee, A. R. Park, J. Shin, S. J. Park and S. Y. Lee, *Biotechnol. J.*, 2016, **11**, 1572–1585.
- 17 V. Štrukil, *ChemSusChem*, 2021, **14**, 330–338.
- 18 L. Zhong, A. Tang, P. Yan, J. Wang, Q. Wang, X. Wen and Y. Cui, *J. Colloid Interface Sci.*, 2019, **537**, 450–457.
- 19 A. Z. Werner, R. Clare, T. D. Mand, I. Pardo, K. J. Ramirez, S. J. Haugen, F. Bratti, G. N. Dexter, J. R. Elmore, J. D. Huenemann, G. L. Peabody, C. W. Johnson, N. A. Rorrer, D. Salvachúa, A. M. Guss and G. T. Beckham, *Metab. Eng.*, 2021, **67**, 250–261.



20 N. I. Kuznetsova, L. I. Kuznetsova, O. A. Yakovina, V. N. Zudin, B. S. Bal'zhinimaev, A. Bhattacharyya and J. T. Walenga, *Ind. Eng. Chem. Res.*, 2020, **59**, 1038–1044.

21 I. Pardo, R. K. Jha, R. E. Bermel, F. Bratti, M. Gaddis, E. McIntyre, W. Michener, E. L. Neidle, T. Dale, G. T. Beckham and C. W. Johnson, *Metab. Eng.*, 2020, **62**, 260–274.

22 Z. Yang, D. Saeki, R. Takagi and H. Matsuyama, *J. Membr. Sci.*, 2020, **595**, 117529.

23 M.-L. Chen, X. Tang, T.-H. Lu, X.-Q. Zhan and Z.-H. Zhou, *J. Coord. Chem.*, 2019, **72**, 1547–1559.

24 S.-M. You, K.-B. Jeong, K. Luo, J.-S. Park, J.-W. Park and Y.-R. Kim, *Anal. Chim. Acta*, 2021, **1151**, 338252.

